NANO LETTERS

2007
Vol. 7, No. 8
2328−2334

Computational Design of an RNA Hexagonal Nanoring and an RNA Nanotube

Yaroslava G. Yingling and Bruce A. Shapiro*

Center for Cancer Research Nanobiology Program, National Cancer Institute, NCI—Frederick, National Institutes of Health, Frederick, Maryland 21702

Received April 25, 2007; Revised Manuscript Received May 25, 2007

ABSTRACT

The combination of computer modeling, RNA structure versatility, and siRNA function can be efficiently used to design an all-RNA nanoparticle capable of siRNA delivery. Here, we present a computational design of an RNA nanoring and a nanotube. An RNA nanoring consists of six simple linear building blocks that are assembled together via known noncovalent loop−loop contacts based on RNAI/RNAII inverse sequences. The helical sequences of the building blocks can include siRNAs for drug delivery.

The rapidly expanding field of nanobiology opens up the possibilities for the development of new methods and therapies that can be used for the diagnosis, prognosis, and treatment of various diseases such as cancer. While an increasing number of novel drugs and therapeutic agents are being discovered, the problem of delivering them specifically to the desired site or cell has not been solved. Nanoparticles are ideal drug delivery devices due to their novel properties and functions and ability to operate at the same scale as biological entities. There are several issues that are crucial for efficient design and drug delivery by nanoparticles, including the efficient attachment of drugs and vectors, controlled drug release, size, toxicity, biodegradability, and activity of the nanoparticle. Moreover, design of nanoparticles can benefit from the understanding and predictability of the molecular interactions within the nanoparticle and between various molecular components. Such interactions can be predicted and examined via computer simulations that would ultimately lead to a better rate of success for the nanoparticle use.

RNA is an attractive molecule for nanodesign,[1] primarily due to its versatility in structure and function. Structurally, RNA has predictable intra- and intermolecular interactions with well-known structural geometry. The RNA strands that consist of adenine (A), guanine (G), cytosine (C), and uridine (U) can naturally or can be programmed to self-assemble via complementary base pairing. The helical region of RNA has a well-known nanometer scale structural geometry; 2.8 nm per helical turn with 11 base pairs and a 2.3 nm diameter. The self-assembly of RNA into complex structures can be facilitated via complementary base pairing or inter- and intramolecular interactions of different single-stranded regions in the RNA including internal bulges and loop motifs and single-stranded overhangs or "sticky ends". Functionally, RNA is the only biopolymer that can carry genetic information and possess catalytic properties. Furthermore, RNA molecular therapy is one of the promising applications for overcoming disease. For example, small interfering RNA (siRNA) can down-regulate genes responsible for cancer, viral pathogenesis, and inflammatory conditions[2,3] and, thus, is very important for target-based drug discovery and development. Synthetic siRNA can be added to cells in order to artificially induce RNA interference and to silence the expression of target genes in a variety of organisms and cell types. siRNA offers an enormous potential as a therapeutic agent with higher specifity, more effectiveness, and less toxic effect than traditional drugs. However, the successful application of siRNA therapeutics depends on efficient delivery to the appropriate cell. Nanoparticles can be used as delivery vehicles for siRNA therapeutics.[4,5] The minimum requirements for such nanoparticles are that they be less than 100 nm in diameter to penetrate cell membranes, have minimal toxicity, and have protection from exonuclease degradation. Hence, a safe and efficient nanoparticle needs to be designed to deliver therapeutic RNAs.

A protein-free RNA induces a minimal immune response and, thereby, reduces antibody production and cell immunity. Thus, all-RNA nanoparticles can be potentially used in long-term treatment of chronic diseases such as cancer, hepatitis B, or AIDS. A limiting factor for RNA nanoparticles is their stability in the bloodstream and nonspecific cellular uptake, posing a requirement of high dosage. However, the relative

* Corresponding author. E-mail: bshapiro@ncifcrf.gov. Telephone: 301-846-5536. Fax: 301-846-5598.

10.1021/nl070984r
Published on Web 07/06/2007

stability can be improved by minimization of the occurrence of single-stranded regions and overhangs in the RNA nanoparticle, chemical modification of the backbone, and addition of proteins, lipids,[2] and polymeric chains.[6,7]

RNA has been demonstrated to be an efficient nanoparticle. A bacteriophage phi29-encoded RNA (pRNA) has been reengineered to form dimers, trimers, rods, and 3D arrays several micrometers in size through interactions of interlocking loops.[8,9] Prominently, a nanoparticle, containing a pRNA trimer as a delivery vehicle, was used to deliver siRNAs and receptor-binding aptamers and has been demonstrated to block cancer development in cell culture and living mice.[4,5] An H-shaped RNA molecular unit built from a portion of the group I intron domain[10−12] has been shown to form oriented filaments.[12,13] Specific RNA nanoarrangements based on HIV dimerization initiation site stem-loops[14,15] were shown to be capable of thermal isomerization to alternative structures.[16] Small structural fragments found in the ribosome and HIV have been used in the design of artificial RNA building blocks, called tectoRNAs.[17] Each tectoRNA contains a right angle motif that forms a 90° angle between adjacent helices, two interacting hairpin loops at the end of each stem, and a 3′ "sticky stem". The hairpin loops direct the formation of the tetramer via formation of specific noncovalent loop−loop interactions, called "kissing loops", and the "sticky stems" further assemble tetramers into complex nanoarrays. These tectoRNAs can be programmed to self-assemble into novel nano- and mesoscale biofabrics with controllable directionality, topology, and geometry.[13,17] In nanobiotechnology, RNA−RNA interactions can guide precise deposition of gold nanoparticles.[18] For example, self-assembling tectoRNA ladders have been shown to induce a precise linear arrangement of cationic gold nanoparticles, demonstrating that RNA can control regular spacing of gold nanoparticles and can act as a nanocrown scaffold.[19]

The general approach used to create RNA nanoparticles and nanomaterials is to take known RNA structures, cut them into the building blocks, and reengineer single-stranded loops and regions to facilitate the desired self-assembly. The self-assembly of all the above-discussed RNA building blocks into nanostructures is mediated by the complementarity of hairpin loops and loop receptors that form noncovalent RNA−RNA interactions. For precise assembly of the RNA building blocks, each of the corresponding complementary loop−loop interactions is uniquely reengineered.

Two main experimental approaches are used for programmable self-assembly of nucleic acids nanostructures:[1] a single-step assembly that is commonly used for DNA nanostructures[20,21] and a stepwise assembly that has been used for RNA nanostructures.[17] In the first approach, all molecules are mixed together, followed by the slow cool annealing procedure. This is only possible if the target building block structure is the most stable one. This approach is, thus, based on the preferential folding of the building blocks at higher temperatures followed by the self-assembly of these building blocks through weaker interactions into final nanostructures at lower temperatures. In the second approach, the building blocks are separately formed at low magnesium concentration in the first step and are then mixed together at high magnesium concentration to form a final nanostructure. This approach is more time-consuming, and the melting temperatures of the building blocks and the final nanostructure should be well separated.

Computer modeling can assist the experimental community with the design of novel nanostructures and with the optimization of the building blocks and final nanostructures according to requirements of the function and fabrication techniques. Moreover, it is a relatively inexpensive and fast way to create different structural designs and assess their properties. Also, computer-aided RNA nanodesign can use a shape-based approach similar to that used for proteins,[22] where the desired shape guides the choice of the specific building blocks.

Our goal is to use the versatility of RNA structure and the importance of siRNA function to create an all-RNA nanoparticle that is capable of siRNA delivery. Also, we would like to examine the possibility of using the single-step fabrication approach. Thus, there are several important points that must be considered. First, the individual building block formation has to be more energetically favorable than noncovalent loop−loop interactions. Second, these noncovalent intermolecular interactions should be experimentally known and stable. Third, we want to design a nanostructure using as few types of simple building blocks as possible to reduce the experimental and fabrication costs.

The RNA motifs for the assembly of the RNA nanoparticle, such as loop−loop complexes or corner elements, can be taken from numerous high-resolution RNA structures determined by NMR or X-ray crystallography. Because loop−loop interactions are commonly used for self-assembly of separate building blocks into superstructures, we examined all known loop−loop complexes. We found that the NMR-determined loop−loop structure of the RNAI/RNAII inverse complex[23] (Figure 1), which has a distinct bend of 120° at the loop−loop helix, can represent corners of the hexameric ring. The advantage of using this loop−loop structure as a corner motif of a hexamer is that individual building blocks can be designed in a very simple form. RNAI and RNAII are antisense and sense plasmid-encoded transcripts that control the replication of the ColE1 plasmid of *Escherichia coli* via duplex formation. This structure has two important structural features: it exhibits a unique bend and all bases participate in base-pairing. Also the bend at the loop−loop complex can be recognized by the "RNA one modulator" (ROM) protein. The binding of the ROM protein to the kissing loop structure reduces the equilibrium dissociation constant of the complex.[24] Also, the inversion of the RNAI/RNAII loop sequences relative to the wild-type sequences makes the complex dissociate 7000 times more slowly than the wild-type and increases the quality of NMR spectra.[25] We subjected this RNAI/RNAII inverse complex to extensive explicit solvent molecular dynamics simulations to check the flexibility and relative stability. During the course of the simulations, all seven base pairs between the loops of the RNAIi and RNAIIi were maintained. The measurement of the angle between the helical stems (Figure 1b) shows that

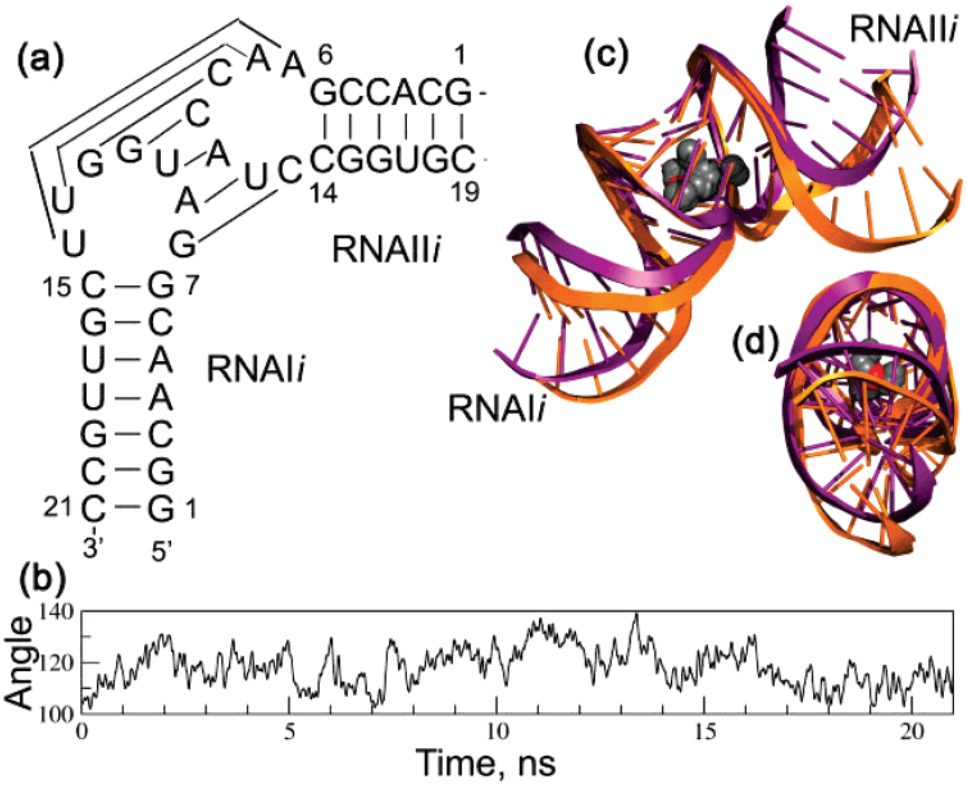

Figure 1. Molecular dynamics simulation of RNAI/RNAII inverse complex. (a) Secondary structure. (b) Temporal angle fluctuations between RNAIi and RNAIIi stems measured during explicit solvent molecular dynamics simulations. (c,d) Superposition of complex's structures at highest (purple) and lowest (orange) angle. The central pocket of the complex is occupied by two Na^+ ions (red) and water molecules (gray).

the structure is stable and fluctuates around a 120° kink at the loop−loop interaction. By superimposing the loop−loop portion of the structure between the highest and the lowest angle, we can observe that the majority of the movement in the angle is mainly due to flexibility of the RNAIIi part of the complex (Figure 1c). However, the movement is of a planar nature (Figure 1d). MD simulations suggest that there is a unique long-residency hydration and cation-binding pocket located in the center of the loop−loop association (Figure 1c,d). The thermodynamic data indicates that the complex formation is accompanied by the uptake of at least two magnesium ions.[26] Computationally observed water and cations have a high occupancy of more than 80% of the trajectory, suggesting that this pocket is probably important in structural stabilization of the complex and could indicate the possible site for magnesium ions uptake. Overall, MD simulations characterize the loop−loop complex as a stable rigid motif with a unique bend and prominent hydration and ion-binding properties. Thus, this loop−loop structure is very well fit to represent the corners of the hexameric ring.

The next step is to create the building blocks using these RNAIi and RNAIIi loops. The simplest approach is to use a helix to connect the desired loops. We designed RNA sequences that form helices capped with the two loops that are based on the RNAIi and RNAIIi sequences (Figure 2). There are two possibilities for forming a ring using RNAIi and RNAIIi loop−loop interactions. The first possibility is to use two types of building blocks, one building block having the RNAIi sequence in both loops (Figure 2a) and

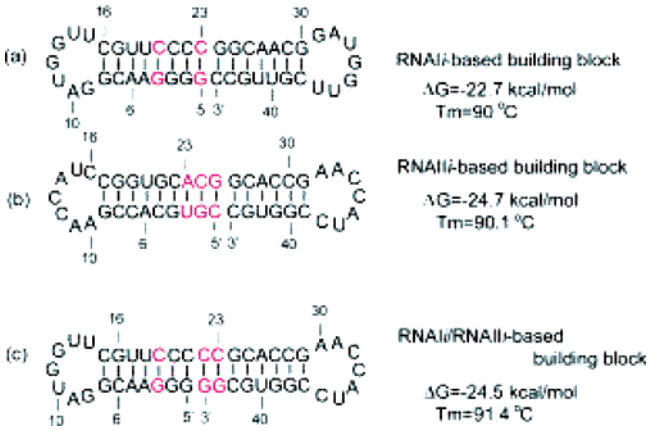

Figure 2. RNA building blocks that contain the sequences from RNAIi and RNAIIi. Free energy was determined using MFOLD.[27] The magenta letters indicate the change made by us to preclude other conformational folds.

the other building block having the RNAIIi sequence in both loops (Figure 2b). The second possibility is to use a single type of building block, where one loop has the RNAIi sequence and the other loop has the RNAIIi sequence (Figure 2c). Using the secondary structure prediction method, MFOLD,[27−29] we modified several base pairs (highlighted in magenta in Figure 2) in each building block in order to obtain the single most energetically favorable structural conformation for a given sequence and thus preclude other conformational folds. Also, the predicted melting temperatures of all the building blocks are around 90 °C and are

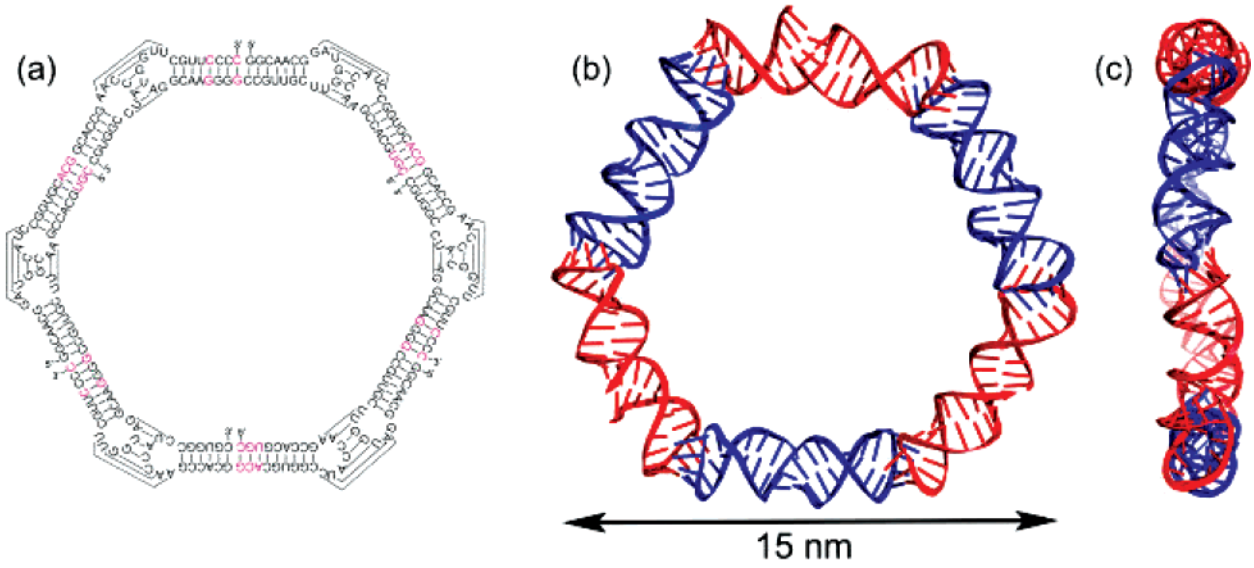

Figure 3. Design of an RNA nanoring from two building blocks. (a) Secondary structure and (b) three-dimensional structure after MD implicit solvent simulations; (b) face view and (c) view from the side.

significantly higher than the determined melting temperature of the RNAI/RNAII inverse loop−loop complex of 59 °C.[26] This large difference in the melting temperatures could permit a slow cool annealing self-assembly of the nanoparticle.

To model the RNA nanoring, we took the original coordinates of the RNAI/RNAII inverse complex and imported it six times into Insight II. To assemble these six-corner complexes into a nanoring, a helical template was used. This helical template has common base pairs with the end of the RNAIi stem at one end and the end of the RNAIIi stem at another end. This template is used to align the corner complexes by superimposing the corresponding common base pairs in the template and the RNAIi stem or the RNAIIi stem. To produce a complete helical turn, three extra base pairs and 3′ and 5′ ends were introduced in the middle of the helical region of a template. The template nucleotides were then removed, leaving a meaningful structure. The rest of the building blocks were fitted in a similar way until a complete nanoring was built. The resultant structure was subjected to slow constrained equilibration and 8 ns implicit molecular dynamics simulations and was shown to possess no violations and was able to maintain stability and planarity. The secondary and tertiary structure of the designed nanoring is shown in Figure 3. Figure 3 shows the minimum size of the nanoring measuring 15 nm diagonally. The size of the ring can be easily expanded by adding full helical turns to the stems of the building blocks. In this case, the size of the nanoring can be easily predicted using the following formula

$$Z = 15 + 2*N*2.8 \text{ [nm]}$$

where Z is the size of the nanoring in nm, N is the number of additional helical turns in the building block, and 2.8 is the length of the full helical turn in nm.

There are at east two possibilities for the potential use of this nanoring for delivery of therapeutic RNAs. The first is to directly include RNA therapeutics into the building block sequences because our nanoparticle is all RNA. The second is to fuse therapeutics onto the 3′ and 5′ ends of the nanoparticle's building blocks.

The structure of a siRNA consists of a short 20−25 nucleotide double strand of RNA with two nucleotide 3′ overhangs at both ends. The siRNA duplex can be generated in situ by cleavage of a short hairpin RNA (shRNA). This shRNA produces a single transcipt, which can be processed into a functional siRNA via an RNA polymerase III promoter.[30] Thus, our building blocks can possess siRNA sequences in the helices closed by RNAIi or RNAIIi loops. There are several factors that are important for the efficient design of shRNA, including the lack of four consecutive adenines (A), to avoid premature transcription termination, an AA flanking dimer on the 5′ end, a G or a C residue after the AA dimer, and sense strand base preferences at positions 3(A), 10(U), 13(A), and 19(A).[31] We can take into account the above-discussed requirements during incorporation of a particular siRNA duplex into the building blocks via use of the RNA secondary structure prediction methods. Thermodynamic experiments indicate that only the sequences of the loops and the first two base pairs in both of the RNAIi and RNAIIi stems are important for the RNAIi/RNAIIi complex stability.[26] However, the rest of the stem's nucleotides do not crucially influence the stability of the complex. Thus, the sequences of the helical part of our building blocks can be engineered into the desired siRNA sequences capping them with RNAIi or RNAIIi loops. The all-RNA nanoring with building blocks containing siRNAs and held together through noncovalent interactions can be used for delivery of therapeutic RNAs. The formation of a tightly folded hexamer with no single-stranded regions should increase the nanoparticle's resistance to exonuclease degradation.[32]

Alternatively or in addition, the constructed nanoring can be used as a polyvalent nanoparticle[9] with six available

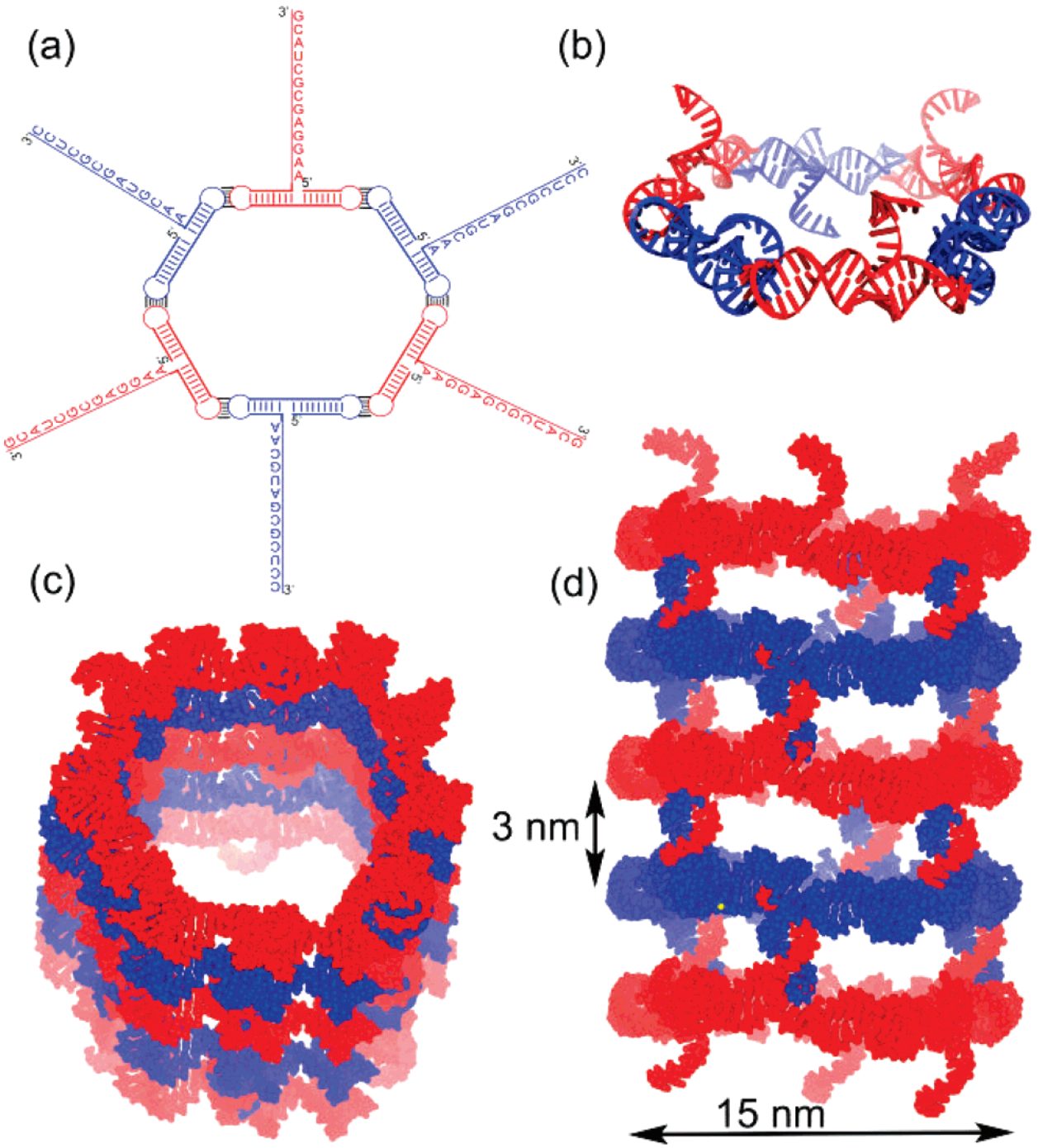

Figure 4. Design of the RNA nanotube. (a) Secondary structure and (b) three-dimensional structure of the nanoring including extensions of the 3′ ends of each building block. Proposed assembly of nanorings into a nanotube via complementary 3′ ends (c) view from the side and (d) view from the top. The rings have identical sequences.

positions at the 3′ and 5′ ends to carry multiple components for cell recognition and therapy, including siRNAs, ribozymes, aptamers, cell surface ligands, heavy metals, quantum dots, and fluorescent beads. It has been shown that connecting the 3′ and 5′ ends of, for example, pRNA building blocks with a ribozyme or siRNA, does not interfere with its folding process and function.[9] Thus, the 3′ and 5′extensions of our nanoring building blocks can potentially be used to bind noncovalently or covalently linked therapeutic RNA sequences, proteins, and molecular beacons. In this design, we extend the 3′ tail using two adenine nucleotides, which have a tendency to turn away from the stem and add 11 bases for a full helical turn (Figure 4a). Three dimensionally, we chose to make breaks (3′ and 5′ ends) in the building block's helices in specific places where the 3′ end of the RNAIi-based building block is facing up and the 3′ end of RNAIIi-based building block is facing down (Figure 4b). If desired, all the tails can face in the same direction by breaking the helices of both building blocks in the same place.

Moreover, we can engineer these 3′ ends to act as sticky, interacting tails that can be programmed to self-assemble into a superstructure. We can design the 3′ tails of the RNAIi-

based building blocks and RNAIIi-based building block to be complementary to each other, thus making the sticky ends that face up from the nanoring to interlock with the sticky ends that face down from another nanoring. Thus, these RNA rings can self-assemble into a nanotube structure (Figure 4c,d) with controllable dimensions.

In conclusion, we describe a shape-based computational approach to build and optimize an all-RNA nanoparticle capable of RNA therapeutics delivery. The RNA nanoring is built from six simple helical building blocks of either one or two types. These building blocks can self-assemble through noncovalent intermolecular interactions, which are well-known for their stability and are based on RNAIi/RNAIIi interactions. The size of the nanoring can be easily extended by incorporation of as many helical turns as needed into the building block helical sequences. Moreover, the incorporation of "sticky ends" into our design allows the design of an RNA nanotube. We have used advanced simulation methods, including secondary structure optimization and explicit and implicit molecular dynamics simulations, to produce a design of a nanoparticle that is able to carry siRNAs. The advantage of the computational approach is that the optimal solution to the desired shape can be determined relatively fast and inexpensively.

Methods. *Three-Dimensional Structure.* The starting coordinates of RNAIi/RNAIIi complex were taken from the PDB Databank (PDB id 2bj2.pdb).[23] The structures were extended and manipulated into a nanoring and nanotube using Insight II and DSViewer.

RNA Secondary Structure Optimization. RNA secondary structure can be predicted from single sequence by free energy minimization methods. The RNA building blocks folding and thermodynamic parameters were determined by the program called MFOLD.[27−29] Alternatively, we can use MPGAfold[33] to determine folding pathways of more complex building blocks.

Molecular Dynamics Simulations. All simulations were performed using the ff99 Cornell force field for RNA,[21,34] which has been shown to be a reliable and refined force field for nucleic acids, and the molecular dynamics software Amber 8.0.[35,36] The explicit solvent method[37] produces the most accurate modeling of solvation effects and can provide crucial information on the direct interactions of water and ions with nucleic acids; however, it is computationally expensive due to the presence of thousands of water molecules. The NMR solution structure of the RNAI/RNAII inverse kissing loop complex was subjected to explicit molecular dynamics simulations. Implicit solvation methods[23] were based on the approximation of electrostatic solvation free energies and permit simulations of larger molecules. The hexagonal RNA ring was subjected to implicit solvent molecular dynamics simulations.

Explicit Solvent. The RNAIi/RNAIIi complex was first neutralized with 38 Na^+ ions. A water box containing 12 565 molecules and an additional 30 Na^+ and 30 Cl^- ions were added to represent a 0.1 M solution. The electrostatic interactions were calculated by particle mesh Ewald summation (PME)[38] and the nonbonded interactions were truncated at 9 Å. The system was minimized first by constraining the solute then the solvent, then heated to 300 K, constraining the RNA then the solvent, and finally equilibrated by slowly releasing the constraints. SHAKE was applied to all hydrogen bonds in the system. Pressure was maintained at 1.0 Pa using the Berendsen algorithm,[39] and a periodic boundary condition was imposed. A production simulation was performed for 13 ns with a 2 fs time step.

Implicit Solvent. The starting nanoring structure was subjected to minimization (10 000 steps), followed by slow 20 kcal/mol constrained heating to 300 K over 200 ps time, and several consecutive MD equilibrations with declining constraints from 2 to 0.1 kcal/mol over a total 500 ps time period. The temperature was maintained at 300 K using a Berendsen thermostat.[39] The monovalent salt concentration was set to 0.5 mol/L. The production simulations were performed for 8 ns using 1 fs time step.

The simulations were carried out on SGI-Altix and SGI-Origin computers using eight processors. The analysis for all simulations was performed using the PTRAJ modules on the production simulations excluding the initial equilibration stage.

Acknowledgment. We have a U.S. Patent pending on the design of the RNA hexagonal nanoring and the RNA nanotube presented in this manuscript. This research was supported by the Intramural Research Program of the NIH, National Cancer Institute, Center for Cancer Research. The computational support was partly provided by the National Cancer Institute's Advanced Biomedical Computing Center.

References

(1) Jaeger, L.; Chworos, A. *Curr. Opin. Struct. Biol.* **2006**, *16*, 531−543.
(2) Yano, J.; Hirabayashi, K.; Nakagawa, S.; Yamaguchi, T.; Nogawa, M.; Kashimori, I.; Naito, H.; Kitagawa, H.; Ishiyama, K.; Ohgi, T.; Irimura, T. *Clin. Cancer Res.* **2004**, *10*, 7721−7726.
(3) Flynn, M. A.; Casey, D. G.; Todryk, S. M.; Mahon, B. P. *J. Inflammation (London)* **2004**, *1*, 4.
(4) Guo, S.; Huang, F.; Guo, P. *Gene Ther.* **2006**, *13*, 814−820.
(5) Khaled, A.; Guo, S.; Li, F.; Guo, P. *Nano Lett.* **2005**, *5*, 1797−1808.
(6) Schiffelers, R. M.; Ansari, A.; Xu, J.; Zhou, Q.; Tang, Q.; Storm, G.; Molema, G.; Lu, P. Y.; Scaria, P. V.; Woodle, M. C. *Nucleic Acids Res.* **2004**, *32* (19), e149.
(7) Howard, K. A.; Rahbek, U. L.; Liu, X.; Damgaard, C. K.; Glud, S. Z.; Andersen, M. O.; Hovgaard, M. B.; Schmitz, A.; Nyengaard, J. R.; Besenbacher, F.; Kjems, J. *Mol. Ther.* **2006**, *14*, 476−484.
(8) Shu, D.; Moll, W.-D.; Deng, Z.; Mao, C.; Guo, P. *Nano Lett.* **2004**, *4*, 1717−1723.
(9) Guo, P. *J. Nanosci. Nanotechnol.* **2005**, *5*, 1964−1982.
(10) Jaeger, L.; Leontis, N. B. *Angew. Chem., Int. Ed.* **2000**, *39*, 2521−2524.
(11) Jaeger, L.; Westhof, E.; Leontis, N. B. *Nucleic Acids Res.* **2001**, *29*, 455−463.
(12) Hansma, H. G.; Oroudjev, E.; Baudrey, S.; Jaeger, L. *J. Microsc.* **2003**, *212* (Part 3), 273−279.
(13) Nasalean, L.; Baudrey, S.; Leontis, N. B.; Jaeger, L. *Nucleic Acids Res.* **2006**, *34*, 1381−1392.
(14) Horiya, S.; Li, X.; Kawai, G.; Saito, R.; Katoh, A.; Kobayashi, K.; Harada, K. *Nucleic Acids Res. Suppl.* **2002**, *2*, 41−42.
(15) Horiya, S.; Li, X.; Kawai, G.; Saito, R.; Katoh, A.; Kobayashi, K.; Harada, K. *Chem. Biol.* **2003**, *10*, 645−654.
(16) Li, X.; Horiya, S.; Harada, K. *J. Am. Chem. Soc.* **2006**, *128*, 4035−4040.
(17) Chworos, A.; Severcan, I.; Koyfman, A. Y.; Weinkam, P.; Oroudjev, E.; Hansma, H. G.; Jaeger, L. *Science* **2004**, *306*, 2068−2072.

(18) Bates, A. D.; Callen, B. P.; Cooper, J. M.; Cosstick, R.; Geary, C.; Glidle, A.; Jaeger, L.; Pearson, J. L.; Proupin-Perez, M.; Xu, C.; Cumming, D. R. *Nano Lett.* **2006**, *6*, 445−448.
(19) Koyfman, A. Y.; Braun, G.; Magonov, S.; Chworos, A.; Reich, N. O.; Jaeger, L. *J. Am. Chem. Soc.* **2005**, *127*, 11886−11887.
(20) Chelyapov, N.; Brun, Y.; Gopalkrishnan, M.; Reishus, D.; Shaw, B.; Adleman, L. *J. Am. Chem. Soc.* **2004**, *126*, 13924−13925.
(21) Mathieu, F.; Liao, S.; Kopatsch, J.; Wang, T.; Mao, C.; Seeman, N. C. *Nano Lett.* **2005**, *5*, 661−665.
(22) Tsai, C. J.; Zheng, J.; Aleman, C.; Nussinov, R. *Trends Biotechnol.* **2006**, *24*, 449−454.
(23) Lee, A. J.; Crothers, D. M. *Structure* **1998**, *6*, 993−1005.
(24) Tomizawa, J. *J. Mol. Biol.* **1990**, *212*, 695−708.
(25) Eguchi, Y.; Tomizawa, J. *J. Mol. Biol.* **1991**, *220*, 831−842.
(26) Gregorian, R. S., Jr.; Crothers, D. M. *J. Mol. Biol.* **1995**, *248*, 968−984.
(27) Zuker, M.; Mathews, D. H.; Turner, D. H. *Algorithms and Thermodynamics for RNA Secondary Structure Prediction: A Practical Guide in RNA Biochemistry and Biotechnology*; Kluwer Academic Publishers: Norwell, MA, 1999.
(28) Zuker, M. *Nucleic Acids Res.* **2003**, *31*, 3406−3415.
(29) Mathews, D. H.; Sabina, J.; Zuker, M.; Turner, D. H. *J. Mol. Biol.* **1999**, *288*, 911−940.
(30) Dykxhoorn, D. M.; Lieberman, J. *Annu. Rev. Med.* **2005**, *56*, 401−423.
(31) Izquierdo, M. *Cancer Gene Ther.* **2005**, *12*, 217−227.
(32) Hoeprich, S.; Zhou, Q.; Guo, S.; Shu, D.; Qi, G.; Wang, Y.; Guo, P. *Gene Ther.* **2003**, *10*, 1258−1267.
(33) Shapiro, B. A.; Bengali, D.; Kasprzak, W.; Wu, J. C. *J. Mol. Biol.* **2001**, *312*, 27−44.
(34) Wang, J. M.; Cieplak, P.; Kollman, P. A. *J. Comput. Chem.* **2000**, *21*, 1049−1074.
(35) Case, D. A.; Darden, T. A.; Cheatham, T. E., III; Simmerling, C. L.; Wang, J.; Duke, R. E.; Luo, R.; Merz, K. M.; Wang, B.; Pearlman, D. A.; Crowley, M.; Brozell, S.; Tsui, V.; Gohlke, H.; Mongan, J.; Hornak, V.; Cui, G.; Beroza, P.; Schafmeister, C.; Caldwell, J. W.; Ross, W. S.; Kollman, P. A. *AMBER 8*; University of California: San Francisco, 2004.
(36) Case, D. A.; Cheatham, T. E., III; Darden, T.; Gohlke, H.; Luo, R.; Merz, K. M., Jr.; Onufriev, A.; Simmerling, C.; Wang, B.; Woods, R. J. *J. Comput. Chem.* **2005**, *26*, 1668−1688.
(37) Auffinger, P.; Westhof, E. *Curr. Opin. Struct. Biol.* **1998**, *8*, 227−236.
(38) Essmann, U.; Perera, L.; Berkowitz, M. L.; Darder, T. A.; Lee, H.; Pedersen, L. G. *J. Chem. Phys.* **1995**, *103*, 8577.
(39) Berendsen, H. J. C.; Postma, J. P. M.; van Gunsteren, W. F.; DiNola, A.; Haak, J. R. *J. Chem. Phys.* **1984**, *81*, 3684−3690.

NL070984R